

Study of Optical Properties of Ag/ZnO Core/Shell Nanoparticles

Himanshu Rajbongshi¹, Suparna Bhattacharjee² and Pranayee Datta³

¹Dept. of Applied Sciences, GUIST, Gauhati University Gauhati University, Guwahati-781014, India

²Dept. of Applied Sciences, GUIST, Gauhati University

³Department of Electronics and Communication Technology, Gauhati University

E-mail: ¹himanshu.rajbongshi31@gmail.com, ²suparnabhattacharjee3@gmail.com

Abstract—In this research work, we report the synthesis of Ag/ZnO core/shell nanoparticles via a simple two step wet chemical method using zinc nitrate hexahydrate [$Zn(NO_3)_2 \cdot 6H_2O$], Potassium hydroxide (KOH) and silver nitrate ($AgNO_3$) as precursors, Polyvinylpyrrolidone (PVP) as capping agent and tri-sodium citrate ($Na_3C_6H_5O_7$) as reducing agent. The structural and optical properties of Ag/ZnO core/shell structure are characterized by scanning electron microscopy (SEM), high-resolution transmission electron microscopy (HRTEM), X-ray diffraction (XRD), ultraviolet-visible spectroscopy (UV-Vis) and photoluminescence (PL) spectroscopy. SEM images reveal that all the Ag nanoparticles and Ag/ZnO core/shell nanoparticles are nearly spherical in shape and uniformly distributed. From HRTEM image, core diameter and shell thickness are found to be 15 nm and 3 nm respectively. XRD pattern of Ag/ZnO core/shell indicates formation of face centred cubic (fcc) structure of Ag NPs and hexagonal wurtzite structure of ZnO. The ZnO shell coating over Ag core results in red shifting of surface Plasmon resonance (SPR) peak of Ag core due to increased refractive index of the surrounding medium. The PL spectroscopy of Ag/ZnO core/shell nanoparticles shows quenching of near band edge emission of ZnO. This is due to the transfer of photogenerated electrons from ZnO shell to the Ag core

Keywords: Core/Shell, HRTEM, red shift, quenching.

1. INTRODUCTION

In recent years, metal/semiconductor core/shell structures have attracted much attention due to their unique optical and electrical properties which have potential applications in photo catalysis [1-4], antibacterial effects [5,6], gas sensors [7,8], fiber optic SPR sensors [9], solar cell and biological sensors [10,11] and so on. Among the semiconductors, ZnO is widely used due to its high (3.37 eV) and direct band gap properties, large binding energy (60 eV), high photocatalytic activity, high physical as well as chemical stability. However rapid recombination of photogenerated electrons and holes in ZnO

lowers its photocatalytic efficiency. To overcome this problem and to increase the photocatalytic efficiency of ZnO, Ag nanoparticles are loaded onto ZnO to form a composite like Ag/ZnO core/shell structure. As conduction band (CB) of ZnO is higher than the fermi-level of Ag, photogenerated electrons in the CB of ZnO get transferred to the Ag core. This enhances the charge separation and prolongs the lifetime of charge carriers. Ag/ZnO core/shell structures have been synthesized by a number of methods, such as Solvothermal methods [12], template-confined synthesis routes [13], low temperature methods [14], hydrothermal synthesis [2] and chemical precipitation methods [15].

In this work, we have synthesized Ag/ZnO core/shell nanoparticles via a simple two step wet chemical method. The Structural and morphological studies confirm the formation of core/shell structure. The optical properties including UV-Visible spectroscopy and Photoluminescence spectroscopy of the synthesized materials are studied and it is found that ZnO shell coating over Ag core results in red shifting of Surface Plasmon resonance (SPR) peak of Ag core due to increased refractive index of the surrounding medium. The PL spectroscopy of Ag/ZnO core/shell nanoparticles shows quenching of near band edge emission of ZnO. This is due to the transfer of photogenerated electrons from ZnO shell to the Ag core.

2. EXPERIMENTAL

2.1 Chemicals and Materials

All materials are purchased from Merck with highest purity (99.99%). Zinc nitrate hexa-hydrate [$Zn(NO_3)_2 \cdot 6H_2O$], Potassium hydroxide (KOH), Polyvinylpyrrolidone (PVP), Silver Nitrate ($AgNO_3$), Tri-sodium Citrate are used as chemical materials for synthesis of Ag nanoparticles and Ag/ZnO core/shell nanoparticles.

2.2 Preparation of Ag nanoparticles

50 ml double-distilled water taken in a 200 ml beaker is allowed to boil at 100°C. Then 20 ml of 0.001M solution of Ag(NO₃)₂ and 10 ml of 0.01 M solution of Tri-sodium citrate are mixed drop wise to the boiling water and stirred constantly at 100°C for 30 min. After 20 minutes the solution becomes green-yellowish which indicates formation of colloidal Ag nanoparticles. The solution is kept undisturbed for 30 min and it turns dark yellowish indicating final formation of Ag NPs and it is allowed to cool at room temperature. The Ag NPs are purified by centrifuging the colloidal solution for 10 min at 10,000 rpm and the obtained precipitate is dispersed in 40 ml double distilled water.

2.3 Preparation of Ag/ZnO core/shell nanoparticles

In order to synthesize Ag/ZnO core/shell structure, 20 ml 0.01M solution of Zn(NO₃)₂.6H₂O is prepared and mixed with 10 ml 2wt % PVP solution. 10 ml of 0.2M KOH solution is prepared and added dropwise to the as synthesized Ag nanoparticles until pH becomes 9. Then Zn (NO₃)₂.6H₂O solution is added dropwise to the mixture and stirred constantly at 80°C for 40 minutes. The solutions after become brownish white in colored are allowed to cool and stored at room temperature for characterization.

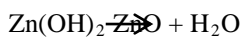
2.4 Characterization methods

Powder X-ray diffraction(XRD) pattern of prepared Ag nanoparticles and Ag/ZnO core/shell nanoparticles are recorded by a Philips X-ray Diffractometer (X'Pert Pro) with Cu K_α1 radiation (λ=1.5406 Å). Surface morphology of the prepared Ag/ZnO nanoparticles is studied using scanning electron microscope (JEOL JSM Model 6390LV). The optical absorption spectra of Ag and Ag/ZnO dispersed in water are recorded by a UV–vis spectrometer (Shimadzu 1800). Photoluminescence spectra are recorded by Hitachi F-2500 fluorescence spectrometer. Transmission electron microscopy (TEM) observations are carried out on a JEM-100 CX II electron microscope.

3. RESULTS AND DISCUSSION

3.1 Growth mechanism of Ag/ZnO core-shell:

ZnO shell is grown over synthesized Ag nanoparticles in aqueous phase by wet chemical method. ZnO nanoparticles are formed in aqueous solutions of Zinc nitrate hexahydrate and KOH according to the following reactions:



Concentration of KOH plays an important role in the formation of ZnO nanoparticles. Higher concentration of KOH

generates excess OH⁻ ions in the solution which combines with Zn(OH)₂ to form [Zn(OH)₄]²⁻ which further involves in the formation of aggregates ZnO nanoparticles. The ZnO nanoparticles aggregate together under the driving forces of surface energy and electrostatic force and a thin layer of ZnO shell is formed on the surface of spherical Ag nanoparticle [2]. With the passage of reaction time ZnO nanoparticles continue to grow on the surface of Ag nanoparticle. With the addition of higher concentration of Zinc nitrate hexahydrate, excess Zn(OH)₂ are formed which helps in the formation of more ZnO nanoparticles and these nanoparticles aggregates on the surface of Ag nanoparticle to form a larger shell of ZnO. Addition of PVP in the solutions prevents Ag/ZnO core-shell nanoparticles to agglomerate.

3.2 Structural characterization

The XRD patterns of pure Ag nanoparticles and Ag/ZnO core/shell nanoparticles are shown in Fig.1. For the Ag NPs, the peaks can be indexed to the face centred cubic(fcc) structure of Ag NP((JCPDS File No. 04-0783). The peaks are (111),(200),(220) and (311). It is also noted that intensity of (111) peak is more intense than the other three peaks indicating that Ag NPs are oriented along this (111) plane. Comparing the intensity of the peaks between the diffraction pattern of Ag NPs and the Ag/ZnO core/shell NPs, it is clear that the intensity of the peaks belonging to the Ag NPs has been reduced in the Ag/ZnO core/shell NPs XRD spectrum. This indicates that Ag NPs are covered with another material. According to the reference code (JCPDS File No. 36-1451) the observed peaks at 2θ values of 31.7, 34.28, 47.4, 56.43, 62.73, 67.8, 72.44 are indexed to the ZnO crystal planes (100), (002), (102), (110), (103), (112), (004) corresponding to hexagonal wurtzite structure of ZnO. Also, no noticeable shift in diffraction peaks of Ag is observed in case of Ag/ZnO core/shell NP which indicates strong interfacial interaction between Ag and ZnO to form core/shell structure.

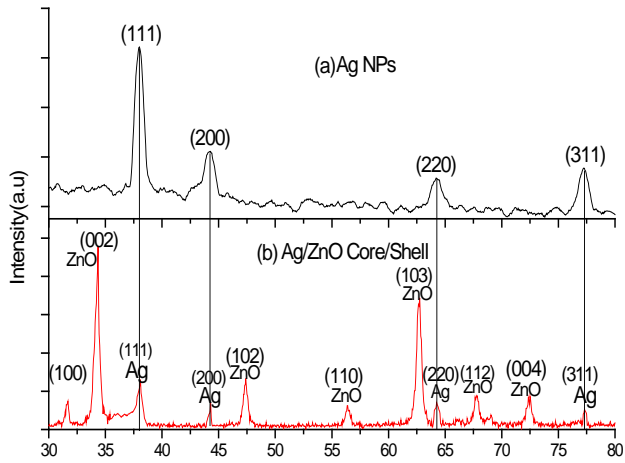


Fig. 1: XRD patterns of the (a) Ag nanoparticles and (b) Ag/ZnO core/shell nanoparticles

3.3. Morphological characterization

From the SEM images of Fig.2, it is seen that all the Ag NPs and Ag/ZnO core/shell NPs are nearly spherical in shape and uniformly distributed.

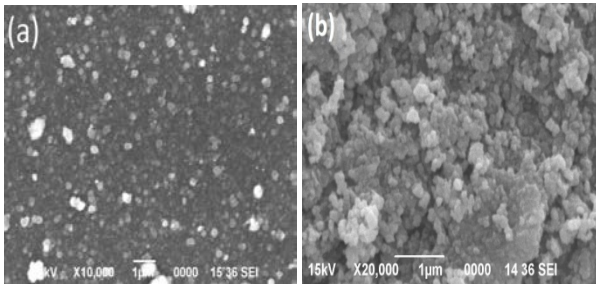


Fig. 2: SEM image of (a) Ag NPs, (b) Ag/ZnO core/shell NPs

Fig. 3(a) shows the TEM image of Ag/ZnO core/shell NPs whereas Fig.3 (b) shows the HRTEM image of single Ag/ZnO core/shell NP. From Fig.3 (b), the core size of Ag nanoparticle is found to be 15.76 nm whereas shell thickness is 3 nm. Ag core is found to have inter planer spacing of about 0.2259 nm which corresponds to the (111) plane of face centered cubic structure and ZnO shell exhibits lattice fringes of spacing of about 0.262 nm which corresponds to the (002) plane of Hexagonal wurtzite structure. In the Fig.3 (d), the SAED pattern shows concentric rings consisting of distinct spots which are due to the presence of many small ZnO nanocrystals and confirm the formation of crystalline ZnO hexagonal phase of Ag/ZnO core/shell structure. In the SAED pattern, there are also spots for Ag, one of which is shown in Fig.3 (d).

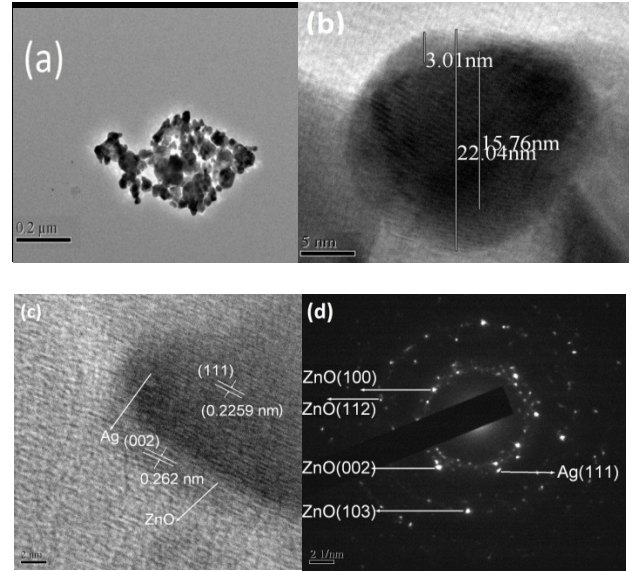


Fig. 3: TEM image of (a) Ag/ZnO core/shell NPs, (b) single Ag/ZnO core/shell NP, (c) lattice fringe pattern of Ag/ZnO core/shell and (d) SAED pattern of Ag/ZnO core/shell NP.

3.4 Optical properties:

UV-Visible spectroscopy:

Fig.4 shows UV-Vis absorption spectra of Ag NPs and Ag/ZnO core/shell NPs. It has been found that Ag NPs show absorption peak at 420 nm whereas in case of Ag/ZnO core/shell structure, the absorption peak becomes broader and show two of them, one at 431 nm and the other at 380 nm. The former absorption peak results due to ZnO shell and the later due to Ag core respectively. It is noticeable that the surface Plasmon resonance (SPR) peak of Ag is red shifted about 11 nm when 3nm ZnO shell is grown over the Ag core. The red shifting in the SPR peak of Ag is due to the increased refractive index of surrounding medium.

The effect of change of refractive index of surrounding medium on the Plasmon resonance wavelength of metal nanoparticle can be qualitatively described as

$\lambda = \lambda_p (2n_0^2 + 1)^{1/2} \approx 3^{1/2} \lambda_p [1 + 1/3(n_0 - 1)]$ [17], where, λ is surface Plasmon wavelength of Ag, λ_p is the bulk plasma wavelength and n_0 is the refractive index of the surrounding medium. As the Ag/ZnO core/shell nanoparticles are dispersed in water medium, the surrounding medium can be considered as a composite of ZnO and water. According to Maxwell-Garnet formula, the effective dielectric constant of this composite layer, ϵ_{eff} can be calculated from $(\epsilon_{eff} - \epsilon_{water}) / (\epsilon_{eff} - 2\epsilon_{water}) = g (\epsilon_{ZnO} - 1) / (\epsilon_{ZnO} + 2)$ [17], where ϵ_{ZnO} is the dielectric constant of ZnO and g is the volume fraction of ZnO shell layer. ϵ_{eff} increases with increase in g value corresponding to the increase of n_0 . As a result, the SPR peak

of Ag nanoparticles gets red shifted continuously with increase of n_0 .

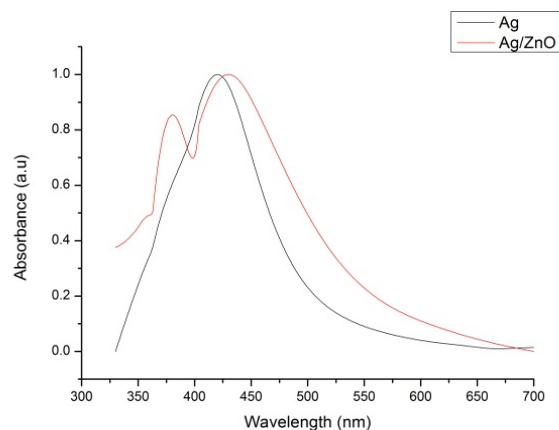


Fig. 4: UV-Vis absorption spectra of Ag NPs and Ag/ZnO core/shell NPs

Photoluminescence study

Usually, there are two kinds of emissions exhibited by ZnO. One is at the ultra-violet range and the other is at the visible range. The near band edge emission originates due to the direct recombination of photo generated electrons in conduction band (CB) and holes in the valence band (VB) and the visible emission is due to the zinc or oxygen vacancy and defect states present in ZnO crystal. When pure ZnO colloidal solution is excited by 330 nm UV light, it shows a near band edge emission peak at 358.62 nm. No visible emission peak is observed which indicates fairly good crystallization and defect free states in ZnO. When Ag/ZnO core/shell structure is excited by 330 nm UV light, it also shows a near band edge emission peak at 358.52 nm but its intensity is less than that for pure ZnO NPs. The reason is as follows: when Ag/ZnO core/shell structure is excited by UV light, photo-generated electron-hole pairs are generated. The photo generated electrons in the VB will be excited to CB leaving same amount of holes in the VB. As the CB of ZnO is higher than the fermi level of Ag, free electrons in the CB of ZnO get transferred to the Ag core continuously until the two systems attain charge equilibrium. It enhances the charge separation and reduces the recombination of photo generated electrons and holes. As a result, the fermi levels of Ag/ZnO core/shell shift closer to the CB of ZnO, thereby quenching the near band edge emission of Ag/ZnO core/shell NPs.

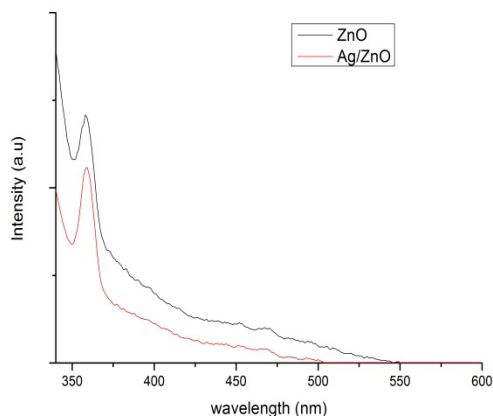


Fig. 5: Photoluminescence spectra of ZnO and Ag/ZnO Core/Shell

4. CONCLUSION

We have successfully synthesized Ag/ZnO core/shell nanoparticles by a facile two step wet chemical method. HRTEM and XRD results confirm the formation and structure of Ag/ZnO core/shell structure. The UV-Vis absorbance spectra shows that coating of ZnO over Ag NP as a shell layer red shifts the position of Surface Plasmon resonance (SPR) absorption of Ag nanoparticle as refractive index of surrounding medium increases. Photoluminescence study suggests that ZnO shell coating over Ag core enhances the charge separation as photo-generated electrons transfer from ZnO shell to the Ag core. As a result of it, the near band edge emission of ZnO gets quenched. This will make the as synthesized sample suitable as photodetector, photocatalyst and solar cell.

5. ACKNOWLEDGEMENT:

The authors acknowledge Department of Chemistry, Gauhati University, Guwahati, for UV-Visible and PL measurements, Dr. Ratan Baruah, Department of Physics, Tezpur University, Tezpur, for XRD and SEM measurements and Regional Sophisticated Instrument Centre, NEHU Shillong for TEM measurements.

REFERENCES

- [1] Jinyan Xiong, Zhen Li, Jun Chen et al. / ACS Appl. Mater. Interfaces 2014, 6, 15716-15725.
- [2] H.R. Liu, G.X. Shao, J.F.Zhao, Z.X.Zhang et al. / J.Phys.Chem.C 2012, 116, 16182-16190.
- [3] Tsutomu Hirakawa and Prashant V. Kamat, J. AM. CHEM. SOC. 2005, 127, 3928-3934.
- [4] Mrinmoy Misra, Pawan kapur, Madan Lal Singla, Applied Catalysis B: Environmental 150-151(2014) 605-611.

-
- [5] Ghosh, S.; Goudar, V. S.; Padmalekha, K. G.; Bhat, S. V.; Indi, S. S.; Vasan, H. N. *RSC Adv.* 2012, 2, 930–940.
- [6] Lu, W. W.; Liu, G. S.; Gao, S. Y.; Xing, S. T.; Wang, J. J. *Nanotechnology* 2008, 19, 445711–445720.
- [7] Simon, Q.; Barreca, D.; Gasparotto, A.; Maccato, C.; Tondello, E.; Sada, C.; Comini, E.; Devi, A.; Fischer, R. A. *Nanotechnology* 2012, 23, 025502.
- [8] Zhu, G. X.; Liu, Y. J.; Xu, H.; Chen, Y.; Shen, X. P.; Xu, Z. *CrystEngComm.* 2012, 14, 719–725.
- [9] A K Sharma and B D Gupta, *J. Opt. A: Pure Appl. Opt.* 9 (2007) 180–185.
- [10] S. Yanagida, Y. Ishimaru, Y. Miyake, T. Shiragami et al. / *Journal of Physical Chemistry* 93 (1989) 2576-2582.
- [11] K. Maeda, K. Teramura, T. Takata et al. / *Journal of Physical chemistry B* 109 (2005) 20504-20510.
- [12] H. Zhai et al. / *Journal of Alloys and Compounds* 600 (2014) 146–150.
- [13] S. Chatterjee et al. / *Journal of Crystal Growth* 312 (2010) 2724–2728.
- [14] G.-H. Shen, F.C.-N. Hong / *Thin Solid Films* 570 (2014) 363–370.
- [15] S. Das et al./*Journal of Photochemistry and Photobiology B: Biology* 142 (2015) 68–76.
- [16] Allen C. Templeton, Jeremy J. Pietron et al. / *J. Phys. Chem. B* 2000, 104, 564-570.
- [17] Yue Zhao, Yanli Ding, Xiang Peng et al. / *Appl Nanosci* 10.1007/s13204-014-0345-y.